

A Simple Synthetic Route for Coordinated Amidine Complexes: a Series of New Anti-tumor Drugs

LIAO Ai-ling^{1,2} ZHOU Xin¹ LI Xiao-dong² XIANG Jing¹

(1. School of Chemistry and Environmental Engineering, Yangtze University, Jingzhou 434020, China;
2. Shenzhen Nanshan People's Hospital, Shenzhen 518052, China)

Abstract In this context, we have provided a facile synthetic route to synthesize the coordinated amidine compounds *via* the *in-situ* reactions of various amines with $[\text{Ru}(\text{salchda})(\text{H}_2\text{O})_2](\text{PF}_6)$ (1) in various nitrile solvents. All the compounds obtained have been well characterized by IR, UV/Vis, CV, ESI/MS, and satisfactory elemental analysis. The crystal structures of a bis(amine) compound and a bis(amidine) ruthenium(III) compound have also determined by X-ray crystallography. These compounds are potential anti-tumor drugs.

Key words amidine complexes; in-situ synthesis; ruthenium complexes; anti-tumor drug

CLC number O641.4

Document code A

0 Introduction

Amidine is a fundamental unit in medicinal and synthetic chemistry that is widely applied in pharmaceutical science and metal complexation ligands^[1-5]. In the past years, great efforts have been focused on developing various new methods to prepare amidine compounds. Although the coordination chemistry of amidine and/or amidinate complexes have been well developed^[6-10], ruthenium amidine complexes remain scarce. However, recent studies have revealed that some amidine (salen)Ru(III) complexes have potential anti-tumor properties^[11]. This series of complexes are cytotoxic against various cancer cell lines, and some complexes have remarkable cancer-cell selectivity. However, the different substituents on the ligand's structures have significant effect on their anti-tumor properties^[12]. Thus, the search for a facile synthetic route to obtain various functionalized amidine complexes is necessary. Herein, we demonstrate that the coordinated nitrile ligands could be readily activated by the (salchda)Ru(III) moiety, which could further react with various amines to generate (salcha)Ru(III) amidine complexes with different substituents.

1 Experimental

1.1 Reagents and instrumentation

The compound *trans*- $[\text{Ru}^{\text{III}}(\text{salchda})(\text{H}_2\text{O})_2]\text{PF}_6$ (1) was synthesized according to literature methods.^[13] $[\text{n-Bu}_4\text{N}]\text{PF}_6$ (Aldrich) for electrochemistry was recrystallized three times from ethanol and dried under vacuum at 120 °C for 24 h. Acetonitrile (Aldrich) for electrochemistry was distilled from calcium hy

收稿日期:2019-10-06

基金项目:国家自然科学基金项目(21771026);南山区科技创新局项目(2018072)资助

通讯作者:向景:男,汉族,博士,教授,研究方向:功能配位材料,E-mail: xiangjing@yangtzeu.edu.cn.

dride. All other chemicals were of reagent grade and used without further purification. All manipulations were performed without the precaution of excluding air or moisture unless otherwise stated. IR spectra were recorded as KBr discs with a Nicolet 360 FTIR spectrophotometer. UV/Vis spectra were recorded with a Perkin-Elmer Lambda 19 spectrophotometer in 1 cm quartz cuvettes. Elemental analysis was performed with an Elementar Vario EL Analyzer. Electrospray ionization mass spectrometry (ESI-MS) was performed with a PE-SCIEX API 365 triple quadrupole mass spectrometer.

1.2 X-ray Crystallography

The data collection for 7 and 8 were carried out with an Oxford CCD diffractometer using graphite-monochromated Mo- K_{α} radiation ($\lambda=0.71073 \text{ \AA}$). Details of the intensity data collection and crystal data are given in Tables 2 and 3. Absorption corrections were carried out by the multi-scan method. The structures were resolved by the heavy atom Patterson method or direct methods and refined by full-matrix least-squares methods by using SHELX-97^[14] and expanded by using Fourier techniques. All non-hydrogen atoms were refined anisotropically. Hydrogen atoms except H1 were generated by the program SHELXL-97. The positions of the hydrogen atoms were calculated on the basis of a riding model with thermal parameters equal to 1.2 times those of the associated carbon atoms and used in the calculation of the final R indices. All calculations were performed by using the teXsan^[15] crystallographic software.

1.3 Synthesis and characterization

[Ru^{III}(Salchda)(NHC(NHCH₂CH₃)CH₃)₂](PF₆) (2). 1 (100 mg, 0.16 mmol) was dissolved in about 25 mL CH₃CN and the solution was refluxed for about 0.5 hour and then ethylamine (0.23 mL, 3.52 mmol) was added into this solution for further refluxed overnight. The solution was concentrated to *ca.* 1 mL. Slow addition of diethyl ether gave a green precipitate which was recrystallized from CH₂Cl₂/diethyl ether. Yield: 56%. IR (KBr, cm⁻¹): ν (N-H) 3361, 3283; ν (C=N) 1633, 1600; ν (P-F) 839. Anal. Calcd. for C₂₈H₄₀N₆O₂PF₆Ru: C, 45.53; H, 5.46; N, 11.38. Found: C, 45.37, H, 5.37, N, 11.19. UV/Vis (CH₃CN): λ_{\max} [nm] (ϵ [mol⁻¹dm³cm⁻¹]) 214(58598), 350(18076), 385(21084), 3613(4067). ESI-MS: $m/z=594$ (M⁺). $\mu_{\text{eff}}=1.949 \mu_{\text{B}}$.

[Ru^{III}(Salchda)(NHC(NHCH(CH₃)₂)CH₃)₂](PF₆) (3). 1 (100 mg, 0.16 mmol) was dissolved in about 25 mL CH₃CN and the solution was refluxed for about 0.5 hour and then isopropylamine (0.30 mL, 3.52 mmol) was added into this solution for further refluxed overnight. The solution was concentrated to *ca.* 1 mL. Slow addition of diethyl ether gave a green precipitate which was recrystallized from CH₂Cl₂/diethyl ether. Yield: 68%. IR (KBr, cm⁻¹): ν (N-H) 3364; ν (C=N) 1632, 1596; ν (P-F) 838. Anal. Calcd. for C₃₀H₄₄N₆O₂PF₆Ru: C, 46.99; H, 5.78; N, 10.96. Found: C, 46.95; H, 5.72; N, 10.80. UV/Vis (CH₃CN): λ_{\max} [nm] (ϵ [mol⁻¹dm³cm⁻¹]) 214(57846), 349(19249), 383(21102), 614(3577). ESI-MS: $m/z=622$ (M⁺). $\mu_{\text{eff}}=1.905 \mu_{\text{B}}$.

[Ru^{III}(Salchda)(NHC(NHC₆H₁₁)CH₃)₂](PF₆) (4). 1 (100 mg, 0.16 mmol) was dissolved in about 25 mL CH₃CN and the solution was refluxed for about 0.5 h and then cyclohexylamine (0.41 mL, 3.52 mmol) was added into this solution for further refluxed overnight. The solution was concentrated to *ca.* 1 mL. Slow addition of diethyl ether gave a green precipitate which was recrystallized from acetone/diethyl ether. Yield: 72%. IR (KBr, cm⁻¹): ν (N-H) 3363, 3272; ν (C=N) 1631, 1613; ν (P-F) 840. Anal. Calcd. for C₃₆H₅₂N₆O₂PF₆Ru: C, 51.06; H, 6.19; N, 9.92. Found: C, 51.06; H, 6.03; N, 10.13. UV/Vis (CH₃CN): λ_{\max} [nm] (ϵ [mol⁻¹dm³cm⁻¹]) 214(62497), 348(22006), 384(23698), 611(4027). ESI-MS: $m/z=702$ (M⁺). $\mu_{\text{eff}}=1.926 \mu_{\text{B}}$.

[Ru^{III}(Salchda)(NHC(NHCH₂Ph)CH₃)₂](PF₆) (5). 1 (100 mg, 0.16 mmol) was dissolved in about 25 mL CH₃CN and the solution was refluxed for about 0.5 hour and then benzylamine (0.39 mL, 3.52

mmol) was added into this solution for further refluxed under argon overnight. The solution was concentrated to *ca.* 1 mL. Slow addition of diethyl ether gave a green precipitate which was recrystallized from CH₂Cl₂/diethyl ether. Yield: 68%. IR (KBr, cm⁻¹): ν (N-H) 3358; ν (C=N) 1630, 1603; ν (P-F) 837. Anal. Calcd. for C₃₈H₄₄N₆O₂PF₆Ru: C, 52.90; H, 5.14; N, 9.74. Found: C, 53.25; H, 4.96; N, 9.44. UV/Vis (CH₃CN): λ_{\max} [nm] (ϵ [mol⁻¹dm³cm⁻¹]) 349(21608), 384(22248), 619(3604). ESI-MS: m/z = 718 (M⁺). μ_{eff} = 1.909 μ_{B} .

[Ru^{III}(Salchda)(NHC(NHCH₂CH₃)Ph)₂](PF₆) (6). Benzonitrile (0.36 mL, 3.52 mmol) was added to a solution of 1 (100 mg, 0.16 mmol) in tetrahydrofuran (15 mL) and the solution was refluxed for about 0.5 h and then ethylamine (0.23 mL, 3.52 mmol) was added into this solution for further refluxed overnight. The solution was concentrated to *ca.* 1 mL. Slow addition of diethyl ether gave a green precipitate which was recrystallized from CH₂Cl₂/diethyl ether. Yield: 46%. IR (KBr, cm⁻¹): ν (N-H) 3363, 3272; ν (C=N) 1631, 1613; ν (P-F) 840. Anal. Calcd. for C₃₈H₄₄N₆O₂PF₆Ru: C, 52.90; H, 5.14; N, 9.74. Found: 52.88; H, 5.21; N, 9.70. UV/Vis (CH₃CN): λ_{\max} [nm] (ϵ [mol⁻¹dm³cm⁻¹]) 218(43742), 231(40575), 352(15352), 385(17636), 633(3806). ESI-MS: m/z = 718 (M⁺). μ_{eff} = 2.048 μ_{B} .

[Ru^{III}(Salchda)(NHC(NHCH(CH₃)₂)Ph)₂](PF₆) (7). Benzonitrile (0.36 mL, 3.52 mmol) was added to a solution of 1 (100 mg, 0.16 mmol) in tetrahydrofuran (15 mL) and the solution was refluxed for about 0.5 hour and then isopropylamine (0.30 mL, 3.52 mmol) was added into this solution for further refluxed overnight. The solution was concentrated to *ca.* 1 mL. Slow addition of diethyl ether gave a green precipitate which was recrystallized from CH₂Cl₂/diethyl ether. Yield: 63%. IR (KBr, cm⁻¹): ν (N-H) 3341, 3248; ν (C=N) 1618, 1601; ν (P-F) 841. Anal. Calcd. for C₄₀H₄₈N₆O₂PF₆Ru: C, 53.93; H, 5.43; N, 9.43. Found: C, 54.77; H, 5.81; N, 9.60. UV/Vis (CH₃CN): λ_{\max} [nm] (ϵ [mol⁻¹dm³cm⁻¹]) 217(68320), 348(23320), 384(23686), 625(3995). ESI-MS: m/z = 746 (M⁺). μ_{eff} = 2.057 μ_{B} .

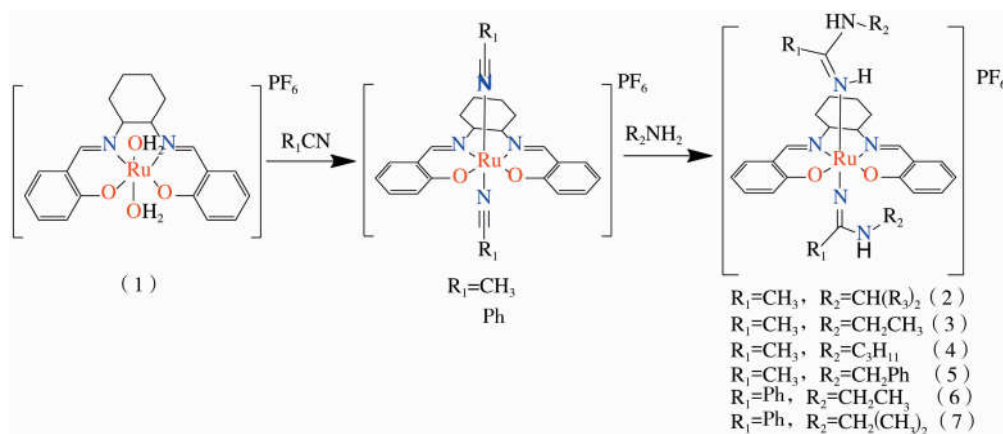
[Ru^{III}(Salchda)(NH₂CH₂Ph)₂](PF₆) (8). Benzylamine (0.39 mL, 3.52 mmol) was added to a solution of 1 (100 mg, 0.16 mmol) in acetone (15 mL). The green solution was refluxed for 1.5 h under argon and then concentrated to *ca.* 1 mL. Slow addition of diethyl ether into the solution gave a green precipitate, which was recrystallized from CH₂Cl₂/diethyl ether. Yield: 72%. IR (KBr, cm⁻¹): ν (N-H) 3312, 3255; ν (C=N) 1596; ν (P-F) 839. Anal. Calcd. for C₃₄H₃₈N₄O₂PF₆Ru: C, 52.31; H, 4.91; N, 7.18. Found: C, 52.01; H, 4.92; N, 7.03. UV/Vis (CH₃CN): λ_{\max} [nm] (ϵ [mol⁻¹dm³cm⁻¹]) 210(56000), 234(38400), 360(14700), 385(18800), 643(4110). ESI-MS: m/z = 636 (M⁺). μ_{eff} = 2.03 μ_{B} .

2 Result and discussion

The diaqua compound, *trans*-[Ru^{III}(salchda)(H₂O)₂](PF₆) (1), was synthesized as the previously reported procedure. Reactions of 1 with various excess amines in ethanol or acetone under Ar afforded various *trans*-[Ru^{III}(salchda)(amine)₂]⁺ compounds in high yields, which were formed by direct substitution of the aqua ligands by amines. However, when CH₃CN were used as solvent instead of ethanol/acetone, the reactions of 1 with amines gave various amidine compounds 2-5 with moderate yields. When benzonitrile was used instead of acetonitrile as the nitrile source, the reactions of 1 with ethylamine or isopropylamine gave the coupling product [Ru^{III}(salchda)(NH=C(NHCH₂CH₃)₂)Ph)₂](PF₆) (6), [Ru^{III}(salchda)(NH=C(NHCH(CH₃)₂)Ph)₂](PF₆) (7), respectively. As shown in Scheme 1, the synthesis of these compounds involves two successive steps. The first step is the substitution of aqua ligands by the solvent nitriles and the second step is nucleophilic addition of amines towards the coordinated organonitrile that was activated by the Ru(III) center.

Obviously, when nitrile is used as solvent, 1 first reacts with the nitrile to form *trans*-[Ru^{III}(salchda)

$(\text{NCR})_2]^+$, which could be validated by ESI/MS in the different reaction time intervals. The coordinated nitriles in the ruthenium(III) salchda complex are found to be electrophilic. The amines which act as nucleophiles then attack the electron deficient α -carbon atoms of the nitrile ligands with the formation of C-N bonds. These bis(amidine)ruthenium(III) compounds are all air-stable. No ligand exchange reaction between the solvent molecules (such as the CH_3CN , benzonitrile and THF) and the amidine ligands was observed for at least 7 days.



Scheme 1 The *in-situ* synthetic routes for various amidine complexes 2-7

In order to validate metal-activated amine-nitrile coupling in this process. Reaction of 1 with ethylamine, isopropylamine and cyclohexylamine in refluxing ethanol solution gave the bis(amine) complexes, respectively. For example, the reaction of 1 with benzylamine in acetone under argon also generated the bis(benzylamine)ruthenium(III) complex 8.

The bis(amidine) compounds 2-7 and bis(amine) compound 8 are paramagnetic and they have room temperature magnetic moments μ_{eff} (solid sample, Gouy method) in the range of 1.91-2.07 μ_{B} , which are consistent with their formulation as low-spin d^5 ruthenium(III) complexes. Infrared spectra (IR) of these bis(amidine) complexes 2-7 show medium ν (N-H) stretches at 3200-3400 cm^{-1} and they also show two sharp peaks around 1630 cm^{-1} and 1600 cm^{-1} , which are partially overlapped. The former peak is assigned to the ν (C=N) stretch of the amidine ligand and the latter one is assigned to ν (C=N) stretch of the salchda ligand. The IR spectrum of the bis(amine)ruthenium(III) complex 8 displays a sharp ν (C=N) stretch around 1600 cm^{-1} and a ν (N-H) stretch around 3300 cm^{-1} . All compounds obtained have a strong broad stretching band at around 840 cm^{-1} , which is attributed to the ν (P-F) stretches of the counter-ion. The ESI-MS of 7 shows a predominant peak at $m/z = 746$, which is assigned to the parent ion $[\text{Ru}^{\text{III}}(\text{salchda})(\text{NH}=\text{C}(\text{NHCH}(\text{CH}_3)_2)\text{Ph})_2]^+$. As shown in Figure 1, the simulated isotopic distribution pattern for m/z 746 is in well agreement with the experimental one. Moreover, there is also a minor peak at $m/z = 584$ due to $[\text{Ru}^{\text{III}}(\text{salchda})(\text{NHC}(\text{NHCH}(\text{CH}_3)_2)\text{Ph})]^+$, which arises from the loss of a benzamidine ligand from the parent ion. The ESI/MS of the other amidine complexes 2-6 have also been investigated in acetone (+ve mode), which are similar to that of 7 and are summarized in the corresponding experimental section. The ESI-MS of bis(amine)Ru(III) compound 8 in acetone exhibit a dominant peak at m/z 636, due to the parent ion.

The UV/Vis spectra of 2-7 in CH_3CN (Table 1) show the strong higher energy absorption bands ($\epsilon \sim 2-6 \times 10^4 \text{ M}^{-1} \cdot \text{cm}^{-1}$) with wavelengths less than 400 nm, which are assigned to the ligand-centered $\pi-\pi^*$ transitions of Schiff bases and amidine ligands. These compounds also show the moderate strong absorption bands in the range of 610-633 nm, which are tentatively assigned to the ligand-to-metal charge transfer (LMCT), possibly mixing with metal-centered (d-d transitions). Compared with these bis(amidine) compounds, the corresponding LMCT absorption bands of 8 is red-shifted and appears at around 640 nm^[16].

The cyclic voltammograms (CV) of 2-8 in CH_3CN show two reversible waves, which are assigned to $\text{Ru}^{\text{IV/III}}$ and $\text{Ru}^{\text{III/II}}$ couples, respectively. As shown in Figure 2(a), the CV of 7 shows two reversible couples centered at $E_{1/2} = 0.38 \text{ V}$ and -1.08 V vs $\text{Cp}_2\text{Fe}^{+/0}$, respectively. Obviously, the redox potentials for these bis(amidine) complexes are similar, but their couples are also sensitive to the axial amidine ligands. When PhCN is used instead of MeCN, both redox couples are shifted to higher potentials, which are in well agreement with that the well π -accepting ligand could stabilize effectively the compounds with the lower oxidation states. For these salchda $\text{Ru}(\text{III})$ compounds with neutral axial ligands, the $\text{Ru}^{\text{III/II}}$ potential increases with the π -accepting ability of the axial ligands. These amino complexes have very closest $\text{Ru}^{\text{IV/III}}$ and $\text{Ru}^{\text{III/II}}$ potentials around $+0.553 \text{ V}$ and -0.950 V vs $\text{Cp}_2\text{Fe}^{+/0}$, Figure 2(b). Compared with the corresponding redox potentials observed in 2-7, both couples are shifted to higher potentials. both couples are shifted to higher potentials, indicating that the axial amidine ligands are better electron-donating ligands than amines.

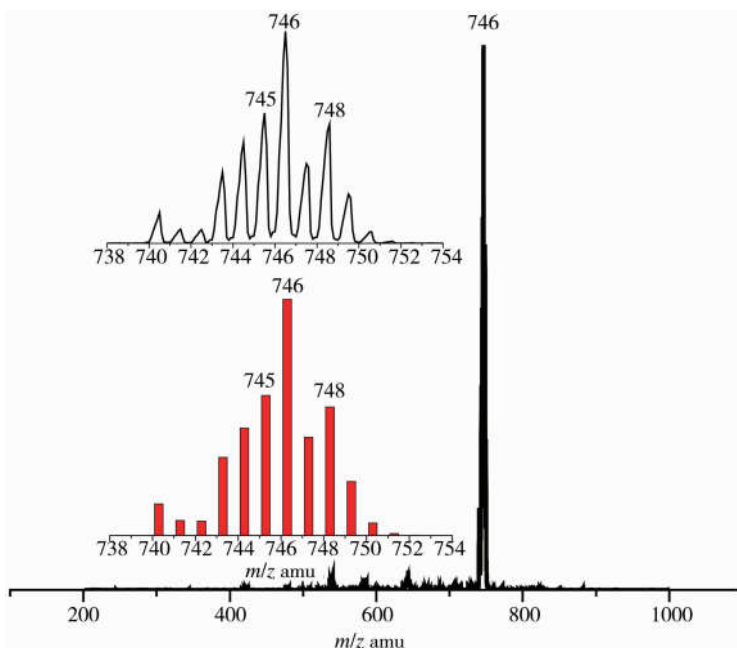


Figure 1 The ESI-MS of 7 in MeOH (Inset: simulated and experimental isotopic distribution patterns of $m/z=746$)

increases with the π -accepting ability of the axial ligands. These amino complexes have very closest $\text{Ru}^{\text{IV/III}}$ and $\text{Ru}^{\text{III/II}}$ potentials around $+0.553 \text{ V}$ and -0.950 V vs $\text{Cp}_2\text{Fe}^{+/0}$, Figure 2(b). Compared with the corresponding redox potentials observed in 2-7, both couples are shifted to higher potentials. both couples are shifted to higher potentials, indicating that the axial amidine ligands are better electron-donating ligands than amines.

Table 1 UV-Vis (CH_3CN) and electrochemical data for complexes 2-8

Complex	λ_{max} (nm (ϵ , $\text{M}^{-1} \cdot \text{cm}^{-1}$))	$E_{1/2}$ (Volts vs. $\text{Cp}_2\text{Fe}^{+/0}$) ^a	
		$\text{Ru}^{\text{IV/III}}$	$\text{Ru}^{\text{III/II}}$
2	214(58590), 350(18070), 385(21080), 613(4060)	0.352	-1.105
3	214(57840), 349(19240), 383(21100), 614(3570)	0.367	-1.131
4	214(62490), 348(22000), 384(23690), 611(4020)	0.365	-1.158
5	349(21600), 384(22240), 619(3600)	0.384	-1.079
6	218(43740), 231(40570), 352(15350), 385(17630), 633(3800)	0.468	-1.004
7	218(68320), 348(23320), 384(23680), 625(3990)	0.428	-1.038
8	210(56000), 234(38400), 360(14700), 385(18800), 643(4110)	0.553	-0.950

Note: a; Glassy carbon working electrode, Pt counter electrode, Ag/AgNO_3 reference electrode, $0.1 \text{ M} [\text{N}^n\text{Bu}_4]\text{PF}_6$ in CH_3CN as supporting electrode. Ferrocene was added as internal standard.

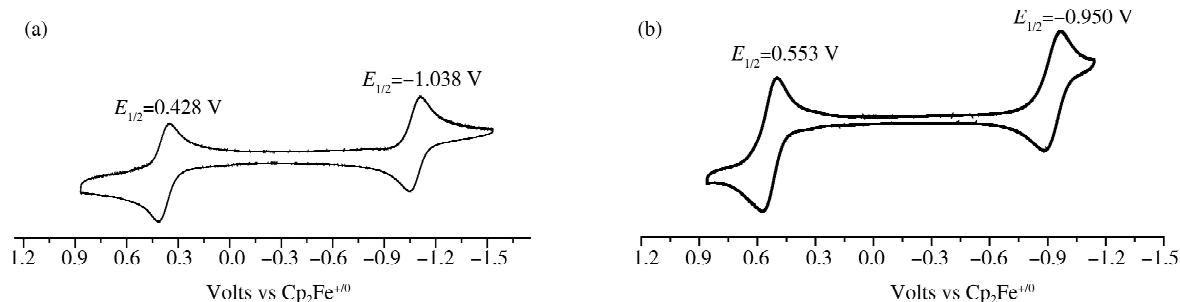


Figure 2 (a) CV of $[\text{Ru}(\text{salchda})(\text{NHC}(\text{NHCH}_2\text{Ph})\text{CH}_3)_2]\text{PF}_6$ (7) in CH_3CN ; (b) CV of $[\text{Ru}(\text{salchda})(\text{NH}_2\text{CH}_2\text{Ph})_2]\text{PF}_6$ (8) in CH_3CN containing $0.1 \text{ M} [\text{N}^n\text{Bu}_4]\text{PF}_6$ (scan rate = 100 mV/S)

The crystal structures of 7 and 8 have been determined by X-ray crystallography. Figure 3a shows the ORTEP diagram of the cation of 7. Selected bond lengths (\AA) and bond angles ($^\circ$) are listed in Table 2 and

3. The compound crystallizes in a monoclinic $C2/c$ space group and features a distorted octahedral geometry. The equatorial bond lengths of Ru-N (1.984(7) Å) and Ru-O (2.029(5) Å) are similar to that of 1. The axial positions are occupied by two *N*-isopropylbenzamidine ligands *via* its imino nitrogen in a *trans* mode. The N-Ru-N bond angle is 178.8(2)°, which is virtually linear. The bond parameters on the amidine ligand are N3-C11=1.303(6) Å, N2-C11=1.323(5) Å and N1-C17-N2=121.12°. These data indicate substantial delocalization of CN₂ group in *N*-isopropylbenzamidine. Intra-molecular H-bonding is observed between N-H of amidine and phenolic oxygen with a distance of 2.852(8) Å.

The ORTEP drawing with partial atom numbering of complex 8 is shown in Figure 3b. The coordination geometry at ruthenium is best described as distorted octahedral structure with two benzylamine molecules occupying the axial position *trans* to each other. One of phenyl group of benzylamine is disordered and six carbon atoms in this phenyl rings are refined with constrained bond parameters. The equatorial position of Ru is taken up by N₂O₂ chromophore. The bond lengths of Ru-N(1.982(4) and 1.990(4) Å) and Ru-O (2.003(3) and 2.011(3) Å) are compared with the known complexes^[17]. The bond lengths of axial Ru-N (2.110(4) and 2.127(4) Å) are obviously longer than the equatorial Ru-N bond lengths. But these bond lengths are slightly shorter than that of the ruthenium (II) species [Ru^{II}(NH₂Ph){PhNC(H)NPh}(Me₂SO)₂Cl] (2.1907(19) Å).^[18] The metrical disparity reflects the *sp*³ and *sp*² nature of the respective coordinated nitrogen.

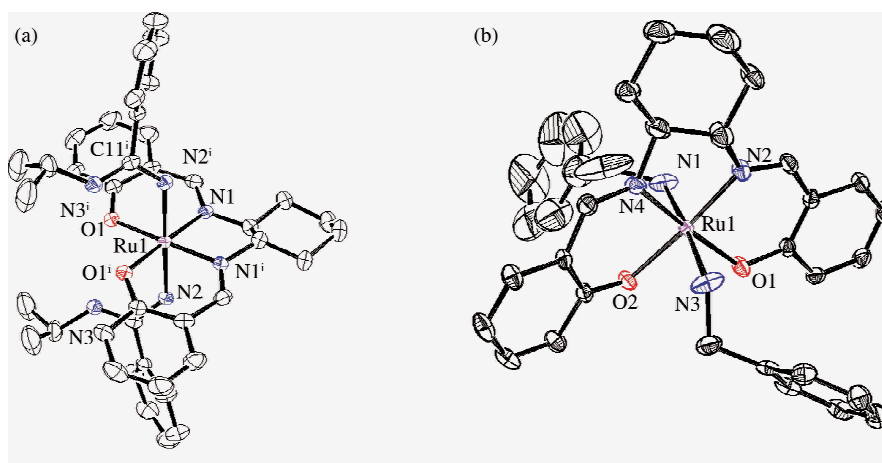


Figure 3 ORTEP drawing of cation of 7 (a) and cationic structure in complex 8 (b) (Thermal ellipsoids are drawn at 30% probability, one of the phenyl rings in 8 is disordered and refined with constrained bond lengths)

Table 2 Selected bond parameter (Å, °) for 7

Bond	Dist. /Å	Bond	Dist. /Å
Ru1-N1	1.987(3)	Ru1-N2	2.059(3)
Ru1-O1	2.027(3)	N3-C11	1.303(6)
N2-C11	1.323(5)		
Angle	/°	Angle	/°
N1-Ru1-N1	83.0(2)	N1-Ru1-O1	176.18(12)
N1-Ru1-O1	93.62(14)	N1-Ru1-O1	93.62(14)
N1-Ru1-O1	176.18(11)	O1-Ru1-O1	89.77(17)
N1-Ru1-N2	93.33(14)	N1-Ru1-N2	85.77(13)
O1-Ru1-N2	88.27(13)	O1-Ru1-N2	92.59(13)
N1-Ru1-N2	85.77(13)	N1-Ru1-N2	93.33(14)
O1-Ru1-N2	92.59(13)	O1-Ru1-N2	88.27(13)
N2-Ru1-N2	178.8(2)		

Table 3 Selected bond length(Å) and bond angle(°) of complex 8

Bond	Dist. /Å	Bond	Dist. /Å
Ru1-N4	1.985(5)	Ru1-O1	2.012(4)
Ru1-N2	1.990(5)	Ru1-N3	2.110(5)
Ru1-O2	2.005(4)	Ru1-N1	2.127(5)
Angle	/°	Angle	/°
N4-Ru1-N2	82.6(2)	O2-Ru1-N3	87.8(2)
N4-Ru1-O2	92.43(18)	O1-Ru1-N3	88.0(2)
N2-Ru1-O1	92.59(18)	N4-Ru1-N1	93.5(2)
O2-Ru1-O1	92.37(16)	N2-Ru1-N1	92.2(2)
N4-Ru1-N3	88.9(2)	O2-Ru1-N1	87.4(2)
N2-Ru1-N3	92.8(2)	O1-Ru1-N1	90.0(2)
N4-Ru1-N2	82.6(2)	O2-Ru1-N3	87.8(2)
N4-Ru1-O2	92.43(18)	O1-Ru1-N3	88.0(2)

Table 4 Crystal data and structure refinement details for 7 and 8

Compound	7	8
formula	C ₄₀ H ₄₈ F ₆ N ₆ O ₂ PRu	C ₃₄ H ₃₈ F ₆ N ₄ O ₂ PRu
Mr	890.88	780.72
cryst syst	Monoclinic	Monoclinic
space group	C 2/c	P 21/c
<i>a</i> /Å	18.7276(10)	11.8056(2)
<i>b</i> /Å	12.8342(6)	15.6521(3)
<i>c</i> /Å	19.7496(10)	17.9313(3)
α	/	/
β	115.179	97.481(2)
γ	/	/
<i>V</i> /Å ³	4295.9(4)	3285.19(10)
<i>Z</i>	4	4
ρ_{calcd} , mg m ⁻³	1.378	1.579
<i>F</i> (000)	1836.0	1596.0
No. of reflns. collected	3800	5783
No. of obsd reflns. (<i>I</i> > 2 σ (<i>I</i>))	2618	4902
Final R indices, <i>I</i> > 2 σ (<i>I</i>) <i>R</i>	0.0491(0.1674)	0.0648(0.1802)
GOF	1.084	1.066
No. of parameters	261	398

3 Conclusion

We have provided a facile synthetic route to obtain various (salchda)Ru(III) bis(amidine) complexes *via* one-pot synthesis with moderate to high yield. The various substituents on the amidine functional group could be tuned by using different nitrile solvent and different amines. These amidine Ru(III) complexes are potential anti-tumor drugs and further works on their application in cell are now in progress.

References

- [1] Greenhill J V, Lue P. Amidines and guanidines in medicinal chemistry [J]. *Prog Med Chem*, 1993, 30: 203-326.
- [2] Ma Y R, De S, Chen C. Syntheses of Cyclic Guanidine-Containing Natural Products [J]. *Tetrahedron*, 2015, 71(8): 1145-1173.
- [3] Guile S D, Alcaraz L, Birkinshaw T N, et al. Antagonists of the P₂X₇ receptor. from lead identification to drug development [J]. *J Med Chem*, 2009, 52(10): 3123-3141.
- [4] Oehlich D, Prokopcova H, Gijsen H J M. The evolution of amidine-based brain penetrant BACE1 inhibitors [J]. *Bioorg Med Chem Lett*, 2014, 24: 2033-2045.
- [5] Oleksyszyn J, Boduszek B, Kam C M, et al. Novel amidine-containing peptidyl phosphonates as irreversible inhibitors for blood coagulation and related serine proteases [J]. *J Med Chem*, 1994, 37(2): 226-231.
- [6] Espirito Santo R D, Machado M G M, dos Santos J L, et al. Use of guanidine compounds in the treatment of neglected tropical diseases [J]. *Curr Org Chem*, 2014, 18(20): 2572-2602.
- [7] Stamford A, Strickland C. Inhibitors of BACE for treating Alzheimer's disease: a fragment-based drug discovery story [J]. *Curr Opin Chem Biol*, 2013, 17(3): 320-328.
- [8] Quek J Y, Davis T P, Lowe A B. Amidine functionality as a stimulus-responsive building block [J]. *Chem Soc Rev*, 2013, 42(17): 7326-7334.
- [9] Taylor J E, Bull S D, Williams J M J. Amidines, isothioureas, and guanidines as nucleophilic catalysts [J]. *Chem Soc Rev*, 2012, 41(6): 2109-2121.

- [10] Greenhill J V, Lue P. Amidines and guanidines in medicinal chemistry [J]. Prog Med Chem, 1993, 30: 203-326.
- [11] Li C, Ip K W, Man W L, et al. Cytotoxic (salen)ruthenium(III) anticancer complexes exhibit different modes of cell death directed by axial ligands [J]. Chem Sci, 2017, 8(10): 6865-6870.
- [12] 李大成, 窦建民. 金属碳硼烷、碳硼烷金属配合物抗肿瘤活性研究进展[J]. 聊城大学学报(自然科学版), 2013, 26(1): 33-39.
- [13] Man W L, Kwong H K, Lam W Y, et al. General Synthesis of (Salen)ruthenium(III) Complexes via N-N Coupling of (Salen)ruthenium(VI) Nitrides [J]. Inorg Chem, 2008, 47(13): 5936-5944.
- [14] Sheldrick G M. SHELXTL Reference Manual [CP]. Version 5.1, Bruker AXS, Madison, WI, 1997.
- [15] teXsan for Windows: Crystal Structure Analysis Package [CP]. Molecular Structure Corporation, 1997.
- [16] Tanabe Y, Kuwata S, Ishii Y. Syntheses and Skeletal Transformations of NCNH- and NCN-Bridged Tetrairidium(III) Cages [J]. J Am Chem Soc, 2002, 124(23): 6528-6529.
- [17] Silva M F C G D, Branco E M P R P, Wang Silva Y, et al. Syntheses and properties of cyanamide and cyanoguanidine complexes of platinum(II). X-Ray structure of trans-[Pt(CF₃)(NCNEt₂)(PPh₃)₂][BF₄][J]. J Organomet Chem 1995, 490(1/2): 89-99.
- [18] Martins L M D R S, Alegria E C B A, Hughes D L, et al. Syntheses and properties of hydride-cyanamide and derived hydrogen-cyanamide complexes of molybdenum(IV). Crystal structure of [MoH₂(NCNH₂)₂(Ph₂PCH₂CH₂PPh₂)₂][BF₄]₂[J]. Dalton Trans, 2003, 33(1): 3743-3750.

脘配合物简易合成路线: 一系列新的抗肿瘤药物

廖爱玲^{1,2} 周鑫¹ 李晓东² 向景¹

(1. 长江大学 化学与环境工程学院, 湖北 荆州 434023; 2. 深圳市南山区人民医院, 广东 深圳 518052)

摘要 我们通过各种胺与[Ru(salchda)(H₂O)₂](PF₆) (1)在各种腈溶剂中的原位反应,提供了合成配位脘配合物一种易途径. 所得到的脘配合物均通过 IR, UV/Vis, CV, ESI/MS 和元素分析进行了充分的表征. 其中一种配位胺和脘配合物的晶体结构也通过 X 射线晶体学确定. 这些配合物是潜在的抗肿瘤药物.

关键词 脘; 原位合成; 钌配合物; 抗肿瘤药物

中图分类号 O641.4

文献标识码 A